coatings

MDPI

Article

Study of the Application of Recycled Gold Nanoparticles in Coatings for Eyewear Lenses

Peter Majerič [1,2], Djuro Koruga [3,4], Zorana Njegovan [3,4], Žiga Jelen [1], Tilen Švarc [1], Andrej Horvat [5] and Rebeka Rudolf [1,2,*]

[1] Faculty of Mechanical Engineering, University of Maribor, 2000 Maribor, Slovenia; peter.majeric@um.si (P.M.); z.jelen@um.si (Ž.J.); tilen.svarc1@um.si (T.Š.)
[2] Zlatarna Celje d.o.o., 3000 Celje, Slovenia
[3] TFT Nano Center, 11050 Belgrade, Serbia; djuro.koruga@gmail.com (D.K.); zorana.jovic@tftnanocenter.rs (Z.N.)
[4] Nano Lab, Faculty of Mechanical Engineering, University of Belgrade, 11120 Belgrade, Serbia
[5] Zepter—Slovenica, 2380 Slovenj Gradec, Slovenia; ahorvat@zepter.si
* Correspondence: rebeka.rudolf@um.si

Abstract: The surface plasmon resonance of gold nanoparticles causes visible light absorption and scattering effects that may be used in optical coatings for eliminating blue light emission from display monitors, for blocking UV light, and for decorative applications. This study examines the achievement of functional properties provided by gold nanoparticles in a commercially established C_{60} fullerene-coated eyewear product. The gold nanoparticles used were sourced from recycling rapid lateral flow tests (LFIA), which use gold nanoparticles as test markers. After the gold's recovery, Ultrasonic Spray Pyrolysis (USP) with freeze-drying was used for the synthesis of new gold nanoparticles, to be used in optical coatings. The gold nanoparticles were examined with SEM, TEM, DLS, zeta potential, BET, and Vis-NIR for characterising their shapes and sizes, as is required for determination of the surface plasmon resonance effect. After applying the newly produced gold nanoparticles with fullerene C_{60} in a combined coating for eyewear lenses, the absorption and transmission of the lenses were determined for establishing changes in the coating's functionality. The results show that enhancing the fullerene C_{60} coating with gold nanoparticles improves light absorption and reflectance for blue and UV light further, which may be evaluated as beneficial for the eyewear user, as the reduction in eye strain is increased due to the coating.

Keywords: gold nanoparticles; fullerene C_{60}; lens; coating; characterisation

check for updates

Citation: Majerič, P.; Koruga, D.; Njegovan, Z.; Jelen, Ž.; Švarc, T.; Horvat, A.; Rudolf, R. Study of the Application of Recycled Gold Nanoparticles in Coatings for Eyewear Lenses. *Coatings* **2023**, *13*, 1666. https://doi.org/10.3390/coatings13101666

Academic Editor: Alexandre Botas

Received: 19 August 2023
Revised: 14 September 2023
Accepted: 21 September 2023
Published: 22 September 2023
Corrected: 20 February 2025

Copyright: © 2023 by the authors. Licensee MDPI, Basel, Switzerland. This article is an open access article distributed under the terms and conditions of the Creative Commons Attribution (CC BY) license (https://creativecommons.org/licenses/by/4.0/).

1. Introduction

Eyewear products have long been used to protect the eyes from environmental hazards, to improve visual acuity and enhance fashion aesthetics. Optical coatings are used to change the absorption, reflection and transmission of light through eyewear lenses, in order to provide surfaces with anti-reflection and high-reflection functionalities, or as colour filters. These coatings are produced with thin layers of metals, metal oxides, fluorides and sulphides. The thin layers provide visual benefits for the eyewear user, such as increased or decreased transmissibility, reduced surface reflections or ghost images, and decreased glare [1]. Colour filters may be used in displays, image sensors, decorative solar panels, light-emitting diodes (LEDs) [2], and in lenses for aiding colour blindness [3].

A new type of functional eyewear is emerging, using active materials for achieving additional functionalities, such as sunlight-activated antifogging [4], passive or user-controlled light transmission and colour states [5]. These active materials may also be nanoparticles [2,4] or electrochromic polymers [5].

Gold nanoparticles (AuNPs) exhibit remarkable optical properties due to surface plasmon resonance (SPR), which is highly dependent on the size, shape, and dielectric properties of the

surrounding medium [6]. Harnessing the SPR effect enables the design of eyewear coatings with superior light absorption and reflection properties. A coating with AuNPs can be tuned as a colour filter, allowing for a selective transmission or absorbance of different wavelengths of light in the optical device (NIR, UV, blue light from displays, or selected colours of the light spectrum), which is also useful in eyewear for compensating for a colour blindness deficiency [2,3,6]. The photothermal effect of light absorption and its dissipation as heat due to SPR may also be used for antifogging functionality in eyewear coatings. When illuminated by sunlight, this coating increases the lens temperature by several degrees above the ambient one, and decreases the nucleation of water vapour, causing a fourfold improvement in the fog resistance and threefold faster defogging of an already fogged-up lens [4]. AuNPs in optical coatings also offer advantages for producing flexible optoelectronics, display technologies and optical sensors, as well as decorations [2–4]. For colour blindness, they are used as optical medical devices in tinted lenses [7,8] and contact lenses [9] that filter the overlapping light wavelength (540–580 nm), and, in turn, activate both cone photoreceptors separately. SPR in AuNPs occurs at a wavelength of 520–580 nm, based on their size [10], resulting in an absorbance peak due to the higher absorption and scattering of visible light [6]. This absorption peak aligns with the overlapping wavelengths of the photoreceptors, making AuNPs useful for tinting lenses to help with colour blindness.

The synthesis of AuNPs can be accomplished through various methods, including chemical reduction, green synthesis, and physical methods like laser ablation [11,12]. Each technique has its advantages and limitations, influencing the size, shape and stability of the AuNPs, which influence their refractive index directly [13]. A method for producing AuNPs is Ultrasonic Spray Pyrolysis (USP), which uses an aqueous precursor with dissolved gold salts. Ultrasound generates micron-sized droplets of this precursor, which are then passed through a tube furnace with a carrier gas, where the AuNPs are formed from the droplets at elevated temperatures in the additional presence of a reaction gas. The AuNPs are collected in a liquid medium with stabilisers, which can be freeze-dried to obtain dried AuNPs in a stabiliser matrix [14].

Gold is a valuable and finite resource. The mining and refining of gold has a significant environmental impact. If we ignore all the other environmental impacts of gold mining and focus on carbon emissions, we see that every kilogram of mined and refined gold produces an equivalent of 16 tons of CO_2. In comparison, every recycled kilogram of gold produces, on average, only the equivalent of 53 kg of CO_2 [15]. As the use of gold nanoparticles in various applications from medical to electronics has increased, it is imperative that robust methods are developed and implemented for the recycling of AuNPs [16]. The recycling of nanogold is crucial for environmental sustainability, resource conservation, energy efficiency and economic growth. By recycling nanogold, we can reduce the environmental impact of gold mining, conserve valuable resources, and contribute to a more sustainable and responsible approach to material usage and waste management.

Another source of gold can also be unused COVID-19 rapid antigen tests. Since the pandemic, a large quantity of unused rapid antigen tests have now expired for usability, which can be recycled to obtain the raw materials for reuse. These tests also use AuNPs as markers for the red-colored control and positive test lines [17]. The sizes of the AuNPs enable them to be bound to the relevant active substances in the test, which interact with the virus and allow them to travel along with the lateral flow of the test medium. The SPR effect of AuNPs then enables these particles to be visible as a red line in the designated locations of the test, revealing the presence of the virus.

Nanoparticles are already being used commercially in eyewear coatings. The lenses of the Zepter International light therapy products under the trademark Bioptron and Hyperlight eyewear products use a coating with carbon nanoparticles of fullerene C_{60}, which creates polarised, polychromatic and incoherent (out-of-phase) light with low energy and with no UV radiation [18,19]. These light properties are found to induce bio-stimulative effects on the eyes, beneficial for a range of vision improvements and complementary treatments with standard ophthalmological methods [20]. The application of this coating

on eyewear produces less eye strain and symptoms typically associated with eye fatigue, as excess light exposure (particularly blue light) may cause photochemical, photomechanical and photothermal retinal damage, as well as influencing overnight melatonin secretion and circadian rhythms [21,22]. As a result, fullerene-coated eyewear products reduce visual discomfort, and thus benefit the cognitive abilities of their users (increased attention capacity, quicker reactions, faster processing of visual information) [23–25].

Eyewear with a combination of fullerene C_{60} and AuNPs may have additional benefits for antifogging lenses (during wearing face masks, for sports use, in the medical, security, energy, chemistry and food industries [4]), improved blocking of blue light emissions from display monitors for reducing eye fatigue, glare reduction, improving sleep, mood disorders and overall health, while also having an added commercial role in broadening the public appeal of these products and the adoption of nanotechnology as a part of everyday items.

The goal of this research was to produce a coating on CR-39 organic eyeglass lenses that is a combination of fullerene C_{60} and recycled AuNPs, and, in the second stage, to carry out the appropriate characterisation and evaluate the added functionality of the lenses. The AuNPs were produced with USP synthesis, intended for the production of large quantities of nanoparticles.

2. Materials and Methods

2.1. Recycling of Nanogold for USP Synthesis

The recovery of nanogold was performed from conjugate pads of expired, unused rapid COVID-19 antigen tests, with a process described in a previous study on recycling rapid antigen tests [17]. The conjugate pads, with a weight of 10 g, were soaked in 50 mL of aqua regia (1:3 ratio of nitric acid (HNO_3) and hydrochloric acid (HCl)) for 30 min, and filtered to remove the conjugate pads from the solution. The ICP measurements of this solution showed a content of 0.1 mg/mL of gold, calculated as a total of 5 mg of gold content. Gold acetate (Au (III) acetate, Surepure Chemetals, Florham Park, NJ, USA) was dissolved in the acidic solution, adding 7.990 g of this gold salt with a 50% Au content. The 50 mL solution then had a Au content of 4 g, and was diluted further with deionised water up to 4 L. The final solution then had a Au concentration of 1 g/L in a total volume of 4 L, prepared for USP synthesis.

2.2. Production of AuNPs for Use in Eyewear Coatings

The AuNPs were produced on a proprietary USP device at Zlatarna Celje d.o.o. The device uses 4 ultrasonic generators, a tube furnace with 4 transport and reaction quartz tubes and a system for nanoparticle collection. The prepared precursor solution, with dissolved Au (III) acetate (concentration of Au = 1 g/L, total volume of 4 L), was used in the 4 ultrasonic generators, with 1 L per generator. The generators produce aerosol droplets from the precursor solution with the use of piezoelectric transducer membranes, submerged below the solution, with a frequency of 1.7 MHz. The aerosol droplets are transported through quartz tubes with an inner diameter of 35 mm using nitrogen (N_2, 99.9%) as the carrier gas, with a flow rate of 6 L/min per tube. Inside the furnace there are three heating zones, each with a length of 50 cm. The three heating zones were set at 130, 250 and 500 °C. After the first heating zone, intended for droplet evaporation, hydrogen gas (H_2, 99.9%) was introduced in the tubes with a flow rate of 4 L/min per tube, for the reactions in the second and third heating zones, necessary for AuNP formation. The AuNPs were collected by passing the gas and particles from the reaction tubes in a total of 3.6 L of deionised water with 4.5 g/L of Polyvinylpyrrolidone (PVP) (Sigma-Aldrich, Shanghai, China), with an average molar mass of 40,000 g/mol. PVP was used as a stabilising agent, for increasing the stability of the AuNPs, preventing their agglomeration. The total duration of the USP production was 6 h for producing AuNPs intended for use in experimental coatings for eyewear lenses. The AuNP suspension produced with these parameters (Au acetate precursor, USP parameters, PVP stabiliser) had a brown colour.

The AuNPs suspension produced by USP was concentrated further by rotary evaporation using a Büchi Rotavapor R-300 (Büchi Labortechnik AG, Flawil, Switzerland). The parameters were: vacuum pressure 25 mPa, evaporation flask rotation speed 200 rpm, bath temperature 50 °C. ICP-OES analysis was used to measure the concentration of Au in the concentrated AuNPs suspension before freeze-drying.

Freeze-drying was performed on a lyophiliser, Labfreez instruments FD-200F SERIES (Labfreez Instruments Group Co., Ltd., Beijing, China). The initial freezing was carried out with a temperature of −40 °C for 8 h, followed by two drying stages, a primary drying stage at 20 °C for 24 h, and a secondary drying stage at 30 °C for 40 h. After a total freeze-drying time of 72 h, the dried AuNPs were embedded in a brownish-coloured PVP stabiliser cake.

The final weight of the prepared dried AuNPs was 480.2 mg in a total weight of PVP and AuNPs of 16.35 g. The weight of AuNPs was determined from the Au concentration of the suspension before drying (133.4 mg/L), as determined by the ICP measurements multiplied by the suspension volume (3.6 L).

2.3. Scanning Electron Microscopy (SEM) of the AuNPs' Suspension

The AuNPs suspension was examined using a Scanning Electron Microscope, (SEM), Sirion 400 NC (FEI Technologies Inc., Hillsboro, OR, USA), with an EDX INCA 350 (Oxford Instruments, Abingdon, UK). The samples were prepared by applying an AuNP suspension droplet with a volume of 5 µL onto a SEM stub holder with graphite tape.

2.4. Transmission Electron Microscopy (TEM) of the Dried AuNPs

The samples of the dried AuNPs were examined with a Transmission Electron Microscope (TEM), JEM-2100HR (JEOL, Tokyo, Japan), with an Energy Dispersive X-ray Spectrometer (EDX) JED-2300T (JEOL, Tokyo, Japan). A small piece of the dry AuNP cake was dispersed in ethanol and applied on a 200 mesh Cu TEM grid with carbon formvar film, and left to dry in a desiccator. The electron accelerating voltage was 200 kV, and the EDX was performed at high resolution, in live time mode, with an acquisition time of 200 s and a probe size of 10 nm.

2.5. Determination of the Sizes and Shapes of the Dried AuNPs from TEM and SEM

The TEM and SEM images were examined with the ImageJ software for determining the diameter, circularity, aspect ratio and roundness of the particles. In total, 600 particles were analysed for statistical relevance of the results.

2.6. Dynamic Light Scattering (DLS) and Zeta Potential Measurements of the Dried AuNPs

The analysis for DLS and zeta potential measurements was conducted on a Malvern Zetasizer Nano ZS instrument (Malvern Panalytical, Worcestershire, UK). A sample was prepared from the dried AuNPs by dispersing the particles in distilled water. The concentration of the prepared suspension was 0.00254 g/mL with a pH level of 2.73. The sample was moved into an omega cuvette and put into a DLS analysis machine. The refractive indices for the suspension material were chosen as gold, and for the suspension liquid as water. The results are reported as a mean value from six measurements.

2.7. Inductively Coupled Plasma-Mass Spectrometry (ICP-MS) of the AuNPs' Suspension

The Au concentration of the suspension was measured with Inductively Coupled Plasma–Mass Spectrometry (ICP-MS), using an HP Agilent 7500 CE spectrometer equipped with a collision cell (Agilent, Santa Clara, CA, USA). The following conditions were used for the ICP-MS: the power was 1.5 kW, Nebuliser–Meinhard, plasma gas flow 15 L/min, nebuliser gas flow 0.85 L/min, make-up gas flow 0.28 L/min, and reaction gas flow 4.0 mL/min. The instrument was calibrated with matrix matched calibration solutions, with an estimated relative measurement uncertainty of ±3%.

2.8. Visible-Near-Infra Red Spectroscopy (Vis-NIR) of the AuNPs

The instrument used for the UV-Vis spectroscopy was an Agilent Cary 60 (Agilent, Santa Clara, CA, USA). A sample was prepared from the dried AuNPs by dispersing the particles in distilled water with a concentration of 0.00912 g/mL. In total, 300 µL of the sample was transferred to a flat-bottomed transparent polystyrene plate for measurements in the light wavelength range of 400–1000 nm.

2.9. Production of CR-39 Lenses with Fullerene C_{60} and AuNPs Coating-Fullerene

Fullerene C_{60} (MST, Riga, Latvia), of purity 99.9%, was mixed mechanically with AuNPs (Zlatarna Celje, Celje, Slovenia) of purity 99.9%. Both materials were in powder form, and the mixture of materials was made at Nano laboratory, University of Belgrade, Serbia using Kenics KM Static Mixer (National Oilwell Varco, Houston, USA) with the conditions: temperature 20 ± 1 °C and humidity 28%.

The mixed nanomaterials (35 wt. % C_{60} molecules and 60 wt. % gold nanoparticles) were then placed in a container that was fixed in the chamber of the vacuum deposition machine (Kenosistec, Binasco, Italy).

Clean CR-39 lenses (Weihai Dingxin Optical, Weihai, China) were placed on the calotte, after which the calotte, with 80 lenses, was placed in the machine for vacuum deposition. Then, the parameters for the production process were assigned to the machine (operating temperature, strength of the ion cannon, thickness of the layers of the neat material, number of passes, thickness of protective layers, etc.). The layering process takes 6–8 h, depending on the parameters set.

2.10. Measurements of Light Intensity Passing through CR-39 Lenses with Fullerene C_{60} and AuNPs Coating

The intensity of light passing through the lenses was measured at Nano laboratory, University of Belgrade, Serbia with a Hamamatsu UV-Vis-NIR spectrometer (200–1100 nm) in real conditions, during a clear, very sunny day without clouds. The variation of sunlight over ten measurements was only 0.8%. The measurements were performed on a lens with a C_{60} coating, a lens with a C_{60} and AuNP coating, two other commercially obtained lenses for comparison, and direct sunlight as the control.

2.11. FTIR Measurements

The FTIR measurements were performed on a Shimadzu IRAffinity-1S device (Shimadzu, Kyoto, Japan). Measurements were performed on the coating and base material using an ATR fixture.

2.12. FIB Measurements of Coating Thickness

An SEM with a Focused Ion Beam (FIB) was used for measuring the produced fullerene C_{60} and AuNPs coating on the lens. A gallium liquid metal ion source on a Quanta 3D (FEI Technologies Inc., Hillsboro, OR, USA) SEM was used for the thickness measurements. The samples were applied on SEM stub holders with conductive carbon adhesive tape, with an additional preparation with Ag paste for increased conductivity for the SEM imaging and FIB cross-section milling. A cross-section with a length of 30 µm, width of 6 µm and a depth of 4 µm was prepared on the coated lens surface.

3. Results

3.1. AuNPs Characterisation

The AuNPs suspension produced from USP had an opaque brown appearance, with a red–violet hue. The total AuNPs suspension in a large container is shown in Figure 1a, while Figure 1b shows the suspension in glass containers, prepared for freeze-drying. From experience obtained with empirical examinations of the AuNPs' synthesis with the proprietary USP device, this colour is apparent after the use of a Au acetate precursor with the selected production parameters. During USP synthesis, the gold-containing precursor

evaporates, forming gold salts, which are reduced to AuNPs, along with the water vapour and acidic constituents. These constituents are then recondensed into the collection medium with PVP. The resulting suspension has a brown colour, as the refraction indexes of the liquid and the SPR of the AuNPs are altered in the water medium with dissolved acetic acid and PVP. The measured concentration of gold in the suspension using the ICP-OES method was 50 µg/mL.

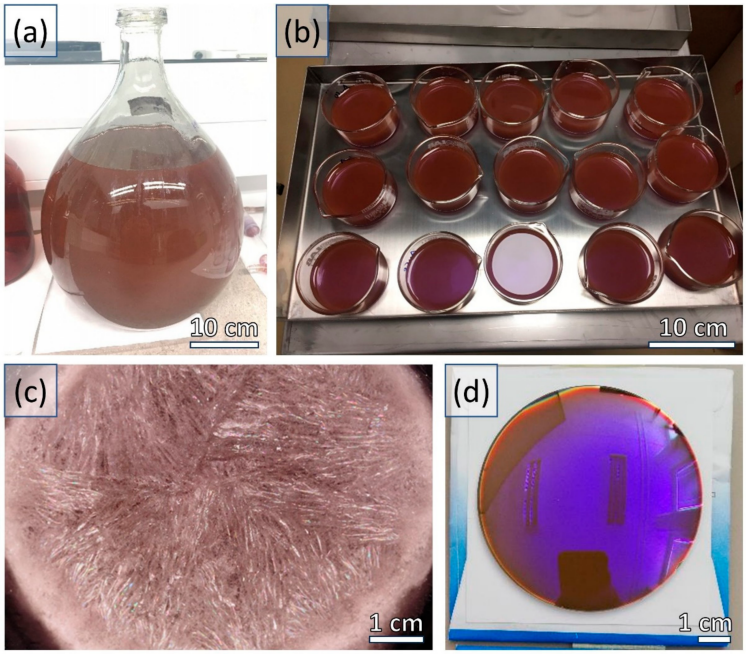


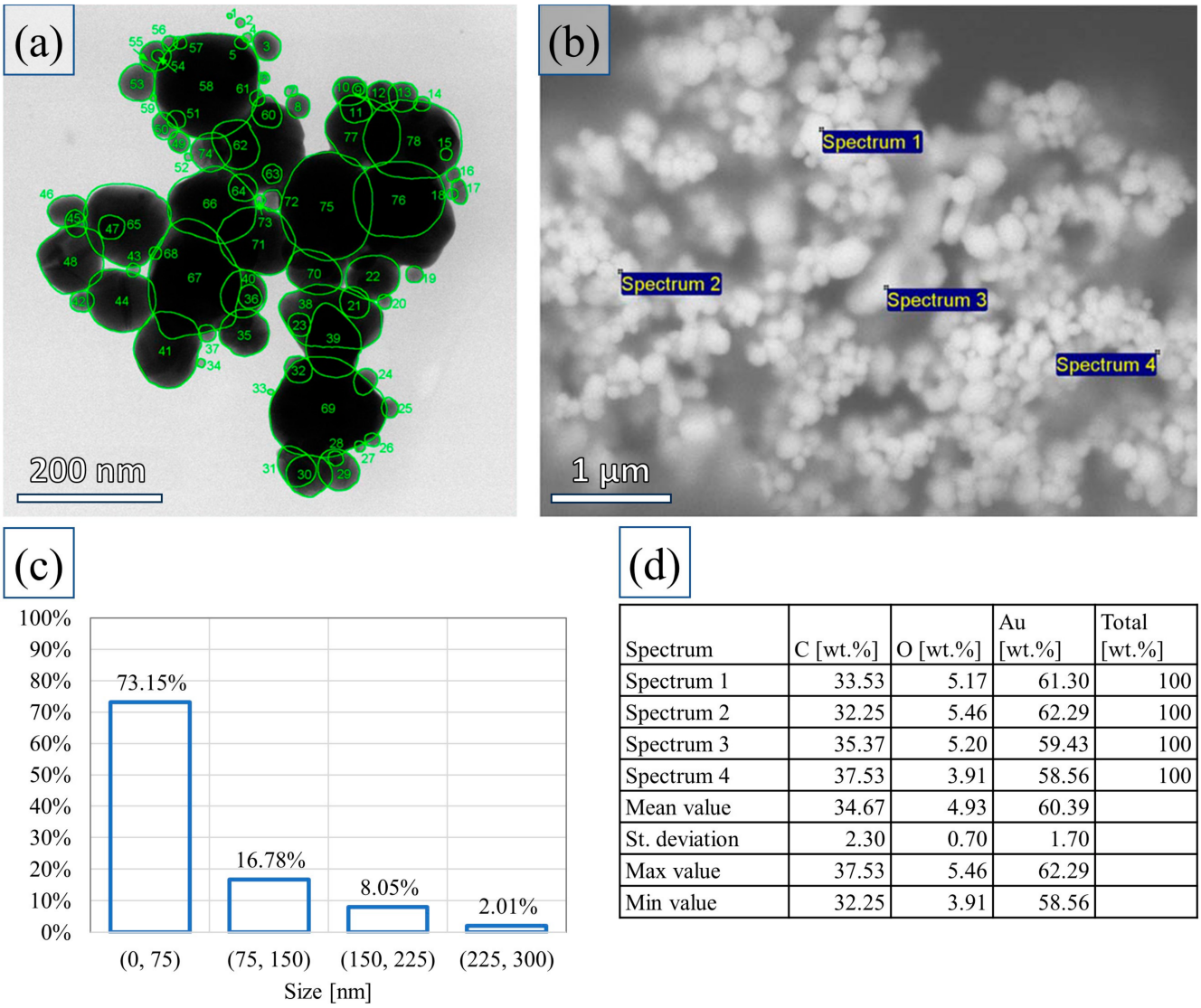
Figure 1. (**a**) Suspension with AuNPs produced by USP. (**b**) AuNPs' suspension, prepared in glass containers for freeze-drying. (**c**) A close-up appearance of one freeze-dried PVP-AuNPs cake, from one glass container. (**d**) A CR-39 lens, coated with AuNPs, prepared for use in an eyewear product.

After freeze-drying, the dried AuNPs and PVP cakes retained a brownish colour, shown in Figure 1c. A brown colour is favourable for incorporation into the eyewear coating, as it does not alter the visual appearance of the final product, shown in Figure 1d. This enables the easier addition of AuNPs on the already commercially established eyewear products. The addition of AuNPs in the coating next to fullerene C_{60}, and their combined benefits for the user, can thus be marketed more effectively.

The SEM and TEM results show somewhat large AuNPs, with sizes of around 150 to 300 nm and several smaller-sized AuNPs. The detailed analysis shows that the smaller particles were present in a greater number than the larger ones. The size distribution was relatively broad, as shown in Figure 2 and detailed in Table 1. An average size of 60 nm was measured, with a standard deviation of 55 nm (60 ± 55 nm). A minimum particle size of 7 nm was measured, indicating the presence of very small particles as well. In total, 73.15% of the measured particles were below 75 nm, as displayed in Figure 1c; 16.78% of the measured particles were in the 75 to 150 nm range, while 10% of the particles were larger, up to 300 nm.

Table 1. Obtained AuNPs' size and morphology parameters: circularity, aspect ratio and roundness.

Measured Value	AuNPs' Diameter (nm)	Circularity	Aspect Ratio	Roundness
Mean value	60.31	0.943	1.147	0.879
Std. Deviation	55.77	0.024	0.112	0.075
Max value	267.97	0.994	1.700	0.986
Min value	7.44	0.842	1.015	0.588



Spectrum	C [wt.%]	O [wt.%]	Au [wt.%]	Total [wt.%]
Spectrum 1	33.53	5.17	61.30	100
Spectrum 2	32.25	5.46	62.29	100
Spectrum 3	35.37	5.20	59.43	100
Spectrum 4	37.53	3.91	58.56	100
Mean value	34.67	4.93	60.39	
St. deviation	2.30	0.70	1.70	
Max value	37.53	5.46	62.29	
Min value	32.25	3.91	58.56	

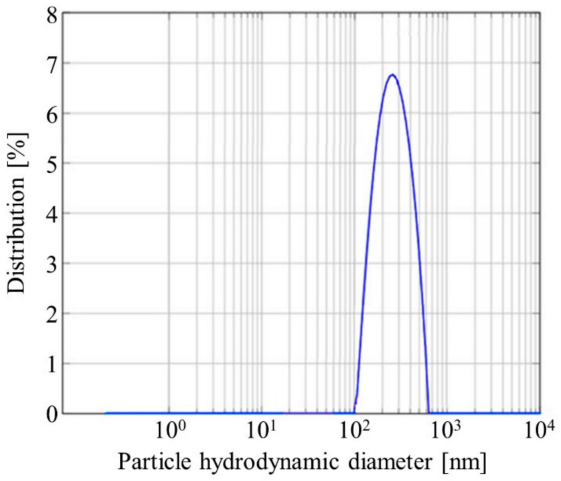
Figure 2. Size, composition and morphology characterisation performed by SEM and TEM. (**a**) TEM image of dried AuNPs with size and morphology analysis. (**b**) SEM image of dried AuNPs with marked locations for EDX analysis. (**c**) Determined particle size distribution from analysing the TEM images. (**d**) EDX results for the selected locations in the SEM image.

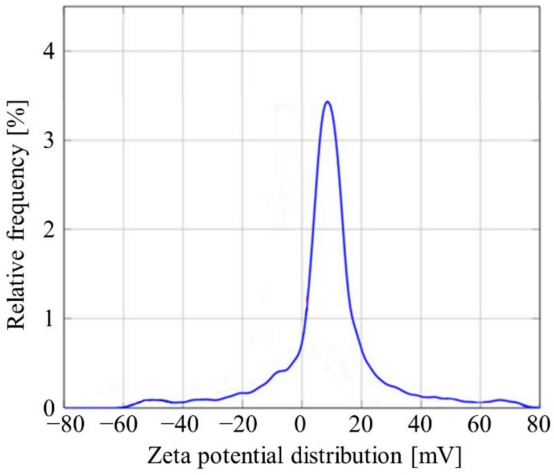
The EDX results from the SEM analysis show the presence of oxygen and carbon along with gold, due to the stabiliser PVP and the underlying graphite tape used for the SEM sample holder. No impurities or contaminations were detected in the samples. The SEM images have patches around the AuNPs, which are not as sharp as practically achievable when imaging the samples. This is due to the influence of the PVP stabiliser, which is not conductive, and affects the imaging adversely. In TEM, this effect was not present, as the dried AuNPs sample was firstly dispersed in ethanol, allowing for thinner sample application on the TEM holder, reducing the effect of the PVP stabiliser's bulk on the imaging.

The AuNPs' morphology analysis from the TEM images showed irregular and spherical particle shapes; in groups they appear as lumps or nuggets. Their shapes were analysed for circularity, roundness and aspect ratio. Circularity was determined in a range of 0–1, where 0 was an elongated particle with jagged edges and 1 was a perfect circle with smooth edges. The measured circularity was 0.943 ± 0.024 (relatively circular with a smooth edge). Roundness ignores the edge smoothness, so it shows how round a particle is from 0 to 1. Roundness is related to the aspect ratio, which is the ratio of the major and minor axes or

diameters of the measured particle. The roundness was 0.879 ± 0.075, and the aspect ratio was 1.147 ± 0.112, indicating particles of a slightly oval shape.

The DLS measurements of the aqueous AuNPs suspension show a hydrodynamic diameter of 267.7 ± 122.8 nm, with a distinct peak at the interval of 100–700 nm in Figure 3. The polydispersion index was relatively low, so we can assume that the particle sizes were not dispersed too broadly. The larger size distributions may be the result of particle clustering and soft agglomeration, as the SEM and TEM measurements showed significantly smaller particles. The smaller particles are also usually visible in the vicinity of the larger particles, which may be a contributing factor for the DLS size measurement results. The zeta potential was measured as being 8.67 ± 0.68 mV, showing low to mid-level stability of the particles, which is an additional reason for the larger particle sizes from the DLS measurements.





Hydrodynamic diameter [nm]	Standard deviation [nm]	Polydispersion index [%]
267.7	122.8	24.74

Average zeta potential [mV]	Standard deviation [mV]	pH
8.67	0.68	2.73

Figure 3. DLS particle size distribution and zeta potential measurements results.

The Vis-NIR measurements performed on the AuNPs' suspensions showed a slight peak for SPR absorption around 531 nm, shown in Figure 4. The SPR effects are thus not greatly expressed. This may be due to the broad size distribution and larger AuNPs present in the suspension, which have diminished SPR properties of light absorption and scattering. An increase in absorption was visible near the infra-red wavelengths and UV wavelengths of light, which may have beneficial effects for application in eyewear products.

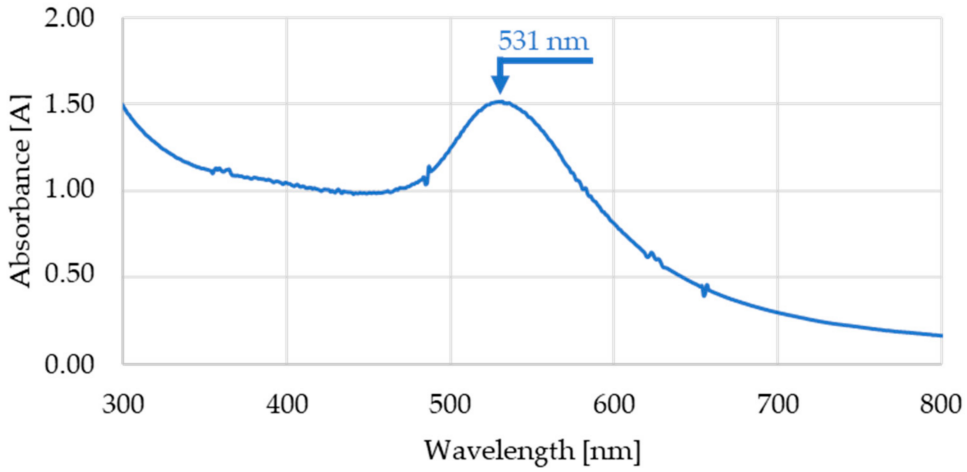


Figure 4. Vis-NIR measurement results with the typical wavelengths for peak SPR absorption at 531 nm.

3.2. Characterisation of a CR-39 Lens with Fullerene C_{60} and AuNPs' Coating

The base layer of a CR-39 lens consists of polyvinyl acetate (PVAc), with typical PVAc peaks at 1735 cm^{-1} (acetate), 1452 and 1398 cm^{-1} (asymmetric C–H bending), 1232 cm^{-1} (C–O asymmetric stretching) and 785 cm^{-1} (O–C=O vibrations), as are visible in Figure 5.

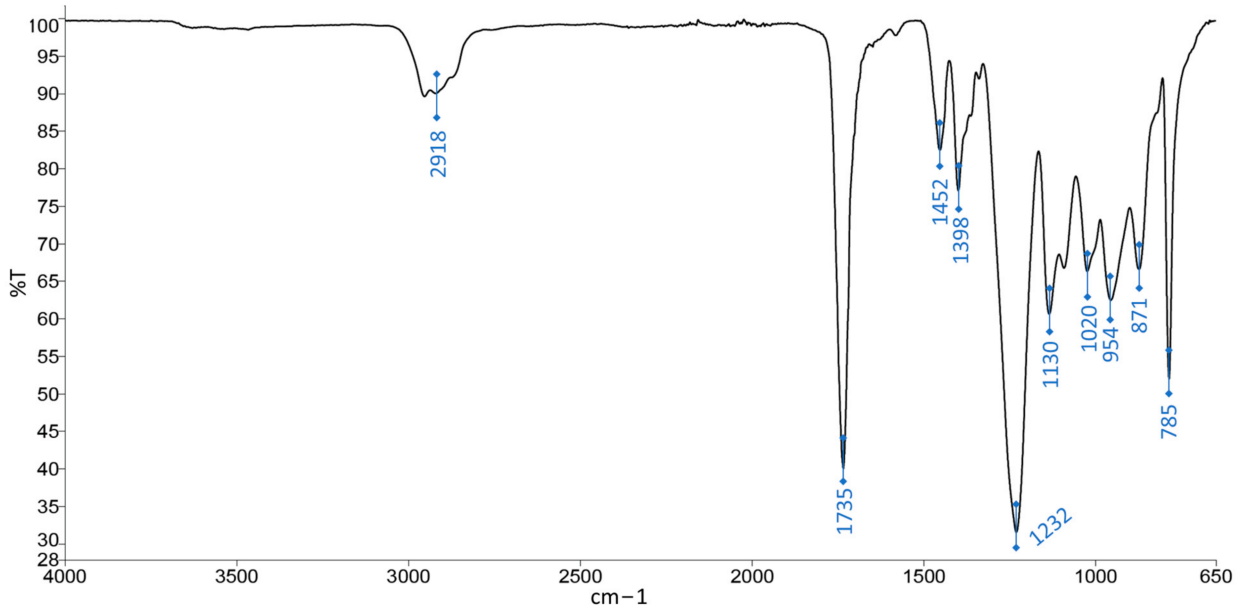


Figure 5. FTIR spectrum of a CR-39 lens.

The coating with fullerene C_{60} and AuNPs blocks all the base layer signal and shows a characteristic peak at 1035 cm^{-1} corresponding to P-O-P or phosphate glass—see Figure 6.

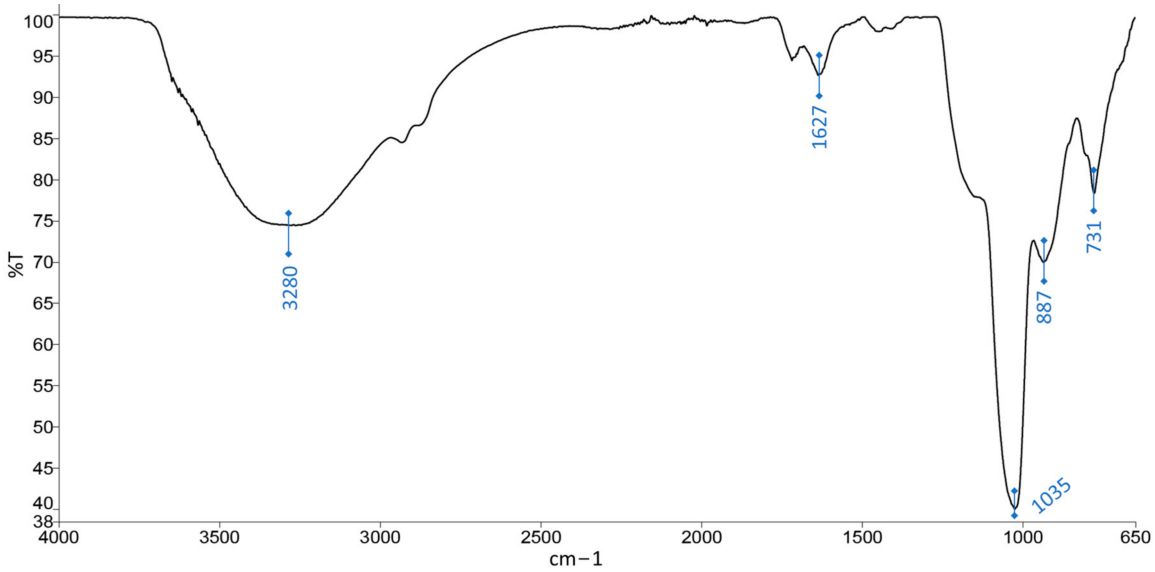


Figure 6. FTIR spectrum of C_{60} and AuNPs coating.

The measured intensity of light (Figure 7) passing through the lens with a fullerene C_{60} and AuNPs coating showed a higher blocking rate of UV, blue light and IR light than the commercially obtained eyewear lenses, marked as M1 and M2. In comparison to the lens with only a fullerene C_{60} coating, the blocking rate is just slightly increased. Based on the effects that these light wavelengths have on well-being, the intensity measurement results of the fullerene C_{60} and AuNPs coating may be interpreted as a small improvement in decreasing eye strain and improving the cognitive abilities of the eyewear user.

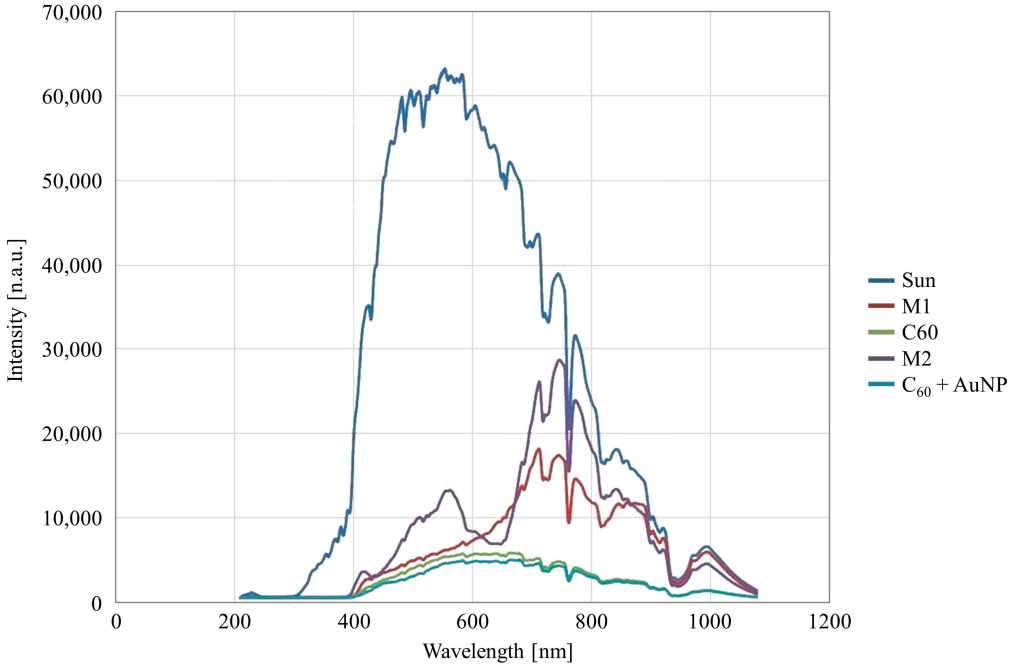


Figure 7. Average light intensity based on ten measurements during a clear sky (sunlight variation 0.8%). Measured light intensity across UV, visible light and NIR wavelengths of a lens with a fullerene C_{60} and AuNPs coating, and commercial eyewear lenses M1 and M2, with a comparison between them and sunlight. The AuNPs have a small effect on the absorption spectra compared with the C_{60} spectra in the range of 400–750 nm.

The FIB-measured thickness of the fullerene C_{60} and AuNPs coating on the surface of the lens was approximately 42–48 nm (Figure 8). The thickness of the coating was smaller than the average sizes of the AuNPs by themselves, indicating that only the smaller-sized AuNPs were incorporated into the final coating. On average, the coating process produced 12 layers of C_{60} (with a diameter of 1 nm), and thus the remaining layers of 30–36 nm thickness are layers of AuNPs. The smallest-sized AuNPs (7.44–10 nm) were incorporated into about three to four layers in the final coating.

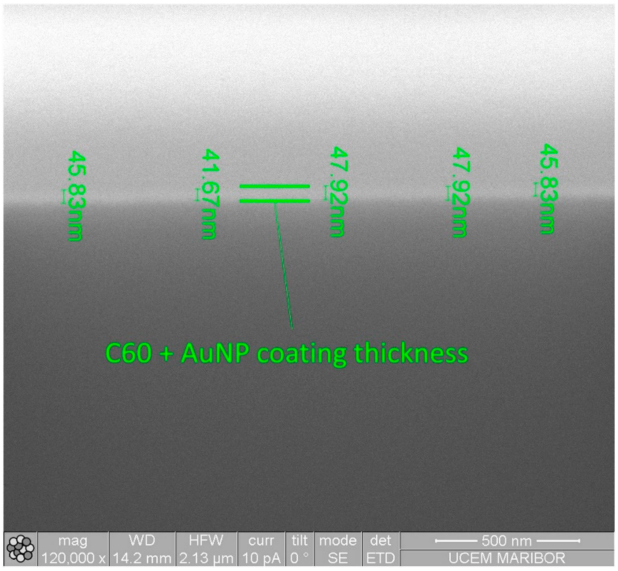


Figure 8. Thickness of the fullerene C_{60} and AuNPs coating on the surface of the lens; cross-section prepared and measured with FIB.

4. Discussion

The produced AuNPs had an opaque brown colour, which is an advantage when using them as additional coating materials in existing eyewear products, which already have a brown colour due to their fullerene coating. The brown colour of AuNP suspensions is not characteristic for mostly spherical AuNP suspensions, which typically have a red to violet colour, depending on their sizes. The change in colour may be attributed to the production route, and subsequent physical and chemical properties of the AuNPs and their surrounding medium. The acetic acid vapours produced during droplet evaporation in the USP process are redissolved in the collection medium, along with the PVP stabiliser. The final combined constituents of the collection medium, along with the AuNPs, result in the brown colour of the suspension and the freeze-dried cakes.

The broad size distribution and particle clustering is another factor in producing the brown colour. As the SPR effect is not demonstrated very strongly by the AuNPs, it is not the dominant factor in the particles' appearance. Larger particles do not contribute greatly to the SPR effects, while smaller ones do. As they are also present in a significant number, a red-violet hue is seen when observing the AuNPs' suspensions in ambient light. Their presence in great volumes was also confirmed in the characterisations. They are usually found in the vicinity of larger particles, which makes them difficult to detect using DLS measurements, which can then only detect the hydrodynamic diameters of particle clusters. The SEM and TEM measurements are more relevant for determining the primary particle sizes, which affect the SPR light absorbance and scattering. The zeta potential also does not show strong particle stability, promoting clustering of the particles, which is another factor to consider in elaborating the AuNPs' properties in regard to their colour and shelf-life when in a suspension form.

A slight peak for SPR absorption at a light wavelength of 531 nm was visible, although it was not very distinct, which may be attributed to a greater rate of agglomeration occurring in the AuNPs suspension. The SEM and TEM images, however, did show clusters of discrete primary particles, and we can estimate that the PVP stabiliser had performed its function. The acid and PVP constituents of the suspension influence the measurements of the particles, resulting in measuring the overall zeta potential and the SPR light absorption of the AuNPs–PVP clusters in the medium.

The measured thickness of the fullerene C_{60} and AuNPs coating showed smaller values than the average sizes of the produced AuNPs. The size distribution, measured from TEM and SEM, showed a great number of nanoparticles smaller than 75 nm, down to 7 nm. During coating production, the larger particles were not incorporated into the coating.

The combined effects of the AuNPs' sizes and shapes, with their surrounding medium (aqueous or dried), give the main property of these particles that is desired for use in the selected existing eyewear product—their brown colour, along with increased absorption in the relevant light wavelengths (UV, blue light, NIR). This makes them beneficial for adding in the combined fullerene C_{60} and AuNPs coatings for eyewear products, for decreasing the eye strain of the users and increasing their overall welfare. Further work is needed for improving the size distributions for increased light absorption effects, while retaining the colour appearance. Incremental improvements in this area are also valuable, as the results may be used for improving the marketability of the coated eyewear products and promoting nanoparticle production technologies in the general population.

5. Conclusions

In summary, the study of the application of recycled AuNPs in coatings for eyewear lenses has demonstrated that the dried AuNPs and PVP cakes after USP synthesis and freeze-drying retained a brownish colour. The recycled AuNPs had an average size of 60 nm, with a standard deviation of 55 nm (60 ± 55 nm). The SEM and TEM analyses showed slightly larger AuNPs with sizes around 150 to 300 nm and several smaller AuNPs. The EDX microchemical analysis did not show the presence of any impurities or contaminations in the AuNPs. The AuNPs' morphology analysis using the TEM Figures showed that they

were irregular in shape, and some spherical particles were also detected. In the AuNPs' groups, their shape was characteristic of agglomerates.

The DLS measurements of the aqueous AuNPs suspension showed a hydrodynamic diameter of 267.7 ± 122.8 nm, with a distinct peak at the interval of 100–700 nm. The larger size distributions may be the result of particle clustering and soft agglomeration. The Vis-NIR measurements performed on the AuNPs suspensions showed a slight peak for SPR absorption around 531 nm.

The coating with fullerene C_{60} and AuNPs blocked all the base layer signal, and showed a characteristic peak at 1035 cm^{-1} corresponding to P-O-P, or phosphate glass. The measured intensity of light passing through the lens with a fullerene C_{60} and AuNPs coating showed a higher blocking rate of UV, blue light and IR light than the commercially obtained eyewear lens. The FIB-measured thickness of the fullerene C_{60} and AuNPs coating on the surface of the lens was approximately 42–48 nm.

Finally, this study provides a comprehensive investigation of the possibility of using AuNPs in optics with the aim of improving the properties of lenses for users.

Author Contributions: Conceptualisation, P.M., D.K. and R.R.; methodology, T.Š., Ž.J. and P.M.; software, T.Š. and Ž.J.; validation, P.M., Ž.J. and R.R.; formal analysis, T.Š., Z.N. and Ž.J.; investigation, P.M., T.Š. and Ž.J.; resources, A.H., D.K. and R.R.; data curation, T.Š., Z.N. and Ž.J.; writing—original draft preparation, P.M.; writing—review and editing, P.M. and R.R.; visualisation, P.M. and T.Š.; supervision, R.R.; project administration, R.R.; funding acquisition, A.H., D.K. and R.R. All authors have read and agreed to the published version of the manuscript.

Funding: This research received external funding from the SPIRIT Slovenia—Public Agency for Entrepreneurship, Internationalization, Foreign Investments and Technology: Agreement P-RRIO-NOO/00042 and from Norway Grants, and a corresponding Slovenian contribution (LFIA-REC, ATP 150).

Institutional Review Board Statement: Not applicable.

Informed Consent Statement: Not applicable.

Data Availability Statement: The data presented in this study are available on request from the corresponding author.

Conflicts of Interest: The authors declare no conflict of interest.

References

1. Citek, K. Anti-Reflective Coatings Reflect Ultraviolet Radiation. *Optom.-J. Am. Optom. Assoc.* **2008**, *79*, 143–148. [CrossRef] [PubMed]
2. Lee, K.-T.; Han, S.Y.; Li, Z.; Baac, H.W.; Park, H.J. Flexible High-Color-Purity Structural Color Filters Based on a Higher-Order Optical Resonance Suppression. *Sci. Rep.* **2019**, *9*, 14917. [CrossRef] [PubMed]
3. Roostaei, N.; Hamidi, S.M. Plasmonic Eyeglasses Based on Gold Nanoparticles for Color Vision Deficiency Management. *ACS Appl. Nano Mater.* **2022**, *5*, 18788–18798. [CrossRef]
4. Haechler, I.; Ferru, N.; Schnoering, G.; Mitridis, E.; Schutzius, T.M.; Poulikakos, D. Transparent Sunlight-Activated Antifogging Metamaterials. *Nat. Nanotechnol.* **2023**, *18*, 137–144. [CrossRef]
5. Österholm, A.M.; Shen, D.E.; Kerszulis, J.A.; Bulloch, R.H.; Kuepfert, M.; Dyer, A.L.; Reynolds, J.R. Four Shades of Brown: Tuning of Electrochromic Polymer Blends toward High-Contrast Eyewear. *ACS Appl. Mater. Interfaces* **2015**, *7*, 1413–1421. [CrossRef]
6. Amendola, V.; Pilot, R.; Frasconi, M.; Maragò, O.M.; Iatì, M.A. Surface Plasmon Resonance in Gold Nanoparticles: A Review. *J. Phys. Condens. Matter* **2017**, *29*, 203002. [CrossRef]
7. Simunovic, M.P. Colour Vision Deficiency. *Eye* **2010**, *24*, 747–755. [CrossRef]
8. Jain, P.K.; Lee, K.S.; El-Sayed, I.H.; El-Sayed, M.A. Calculated Absorption and Scattering Properties of Gold Nanoparticles of Different Size, Shape, and Composition: Applications in Biological Imaging and Biomedicine. *J. Phys. Chem. B* **2006**, *110*, 7238–7248. [CrossRef]
9. Salih, A.E.; Elsherif, M.; Alam, F.; Yetisen, A.K.; Butt, H. Gold Nanocomposite Contact Lenses for Color Blindness Management. *ACS Nano* **2021**, *15*, 4870–4880. [CrossRef]
10. Haiss, W.; Thanh, N.T.K.; Aveyard, J.; Fernig, D.G. Determination of Size and Concentration of Gold Nanoparticles from UV−Vis Spectra. *Anal. Chem.* **2007**, *79*, 4215–4221. [CrossRef]
11. Hu, X.; Zhang, Y.; Ding, T.; Liu, J.; Zhao, H. Multifunctional Gold Nanoparticles: A Novel Nanomaterial for Various Medical Applications and Biological Activities. *Front. Bioeng. Biotechnol.* **2020**, *8*, 990. [CrossRef] [PubMed]

12. Hammami, I.; Alabdallah, N.M.; Jomaa, A.A.; Kamoun, M. Gold Nanoparticles: Synthesis Properties and Applications. *J. King Saud Univ.-Sci.* **2021**, *33*, 101560. [CrossRef]
13. Chen, H.; Kou, X.; Yang, Z.; Ni, W.; Wang, J. Shape- and Size-Dependent Refractive Index Sensitivity of Gold Nanoparticles. *Langmuir* **2008**, *24*, 5233–5237. [CrossRef]
14. Jelen, Ž.; Majerič, P.; Zadravec, M.; Anžel, I.; Rakuša, M.; Rudolf, R. Study of Gold Nanoparticles' Preparation through Ultrasonic Spray Pyrolysis and Lyophilisation for Possible Use as Markers in LFIA Tests. *Nanotechnol. Rev.* **2021**, *10*, 1978–1992. [CrossRef]
15. Fritz, B.; Aichele, C.; Schmidt, M. Environmental Impact of High-Value Gold Scrap Recycling. *Int. J. Life Cycle Assess* **2020**, *25*, 1930–1941. [CrossRef]
16. Oestreicher, V.; García, C.S.; Soler-Illia, G.J.A.A.; Angelomé, P.C. Gold Recycling at Laboratory Scale: From Nanowaste to Nanospheres. *ChemSusChem* **2019**, *12*, 4882–4888. [CrossRef] [PubMed]
17. Švarc, T.; Majerič, P.; Feizpour, D.; Jelen, Ž.; Zadravec, M.; Gomboc, T.; Rudolf, R. Recovery Study of Gold Nanoparticle Markers from Lateral Flow Immunoassays. *Materials* **2023**, *16*, 5770. [CrossRef]
18. Koruga, D. Optical Filter Based on LIGHT-matter Coupling in Quantum-Confined Cavity Spaces, PCT/EP2019/065365. U.S. Patent Application No. 17/595,615, 18 August 2022.
19. Koruga, D. Optical Filter and Method of Manufacturing an Optical Filter. U.S.Patent 11,067,730 B2, 20 July 2021.
20. Jankov, M.R.; Jaksic, V.Z.; Koruga, D. Clinical impact of nanophotonic blue-light filtering spectacles based on fullerene C60 and polymethyl methacrylate (PMMA). *Vojnosanit. Pregl.* **2021**, *78*, 403–408. [CrossRef]
21. Lin, J.B.; Gerratt, B.W.; Bassi, C.J.; Apte, R.S. Short-Wavelength Light-Blocking Eyeglasses Attenuate Symptoms of Eye Fatigue. *Investig. Opthalmol. Vis. Sci.* **2017**, *58*, 442. [CrossRef]
22. Ostrin, L.A. Ocular and Systemic Melatonin and the Influence of Light Exposure. *Clin. Exp. Optom.* **2019**, *102*, 99–108. [CrossRef]
23. Gulyar, S.A.; Filimonova, N.B.; Makarchuk, M.Y.; Kryvdiuk, Y.N. Ocular Influence of Nano-Modified Fulleren Light: 1. Activity of Default Networks of the Human Brain. *J. US-China Med. Sci.* **2019**, *16*, 45–54. [CrossRef]
24. Gulyar, S.A.; Filimonova, N.B.; Makarchuk, M.Y.; Krivdiuk, Y.N. Ocular Influence of Nano-Modified Fullerene Light, 2: Time Correlation of the Choice and Simple Sensorimotor Reactions That Determine Blinding Compensation of the Driver. *J. US-China Med. Sci.* **2019**, *16*, 105–115. [CrossRef]
25. Gulyar, S.A.; Tamarova, Z.A.; Kirilenko, Y.K. Ocular Influence of Nano-Modified Fullerene Light: 3. Speed and Quality of Visual Information Processing in Man. *J. US-China Med. Sci.* **2019**, *16*, 116–133. [CrossRef]

Disclaimer/Publisher's Note: The statements, opinions and data contained in all publications are solely those of the individual author(s) and contributor(s) and not of MDPI and/or the editor(s). MDPI and/or the editor(s) disclaim responsibility for any injury to people or property resulting from any ideas, methods, instructions or products referred to in the content.